EXAMINING THE DISTRIBUTION AND CONCENTRATION OF CARBON ON MERCURY'S SURFACE.

Rachel L. Klima (Rachel.Klima@jhuapl.edu)[1], David T. Blewett[1], Brett W. Denevi[1], Carolyn M. Ernst[1], Scott L. Murchie[1], and Patrick N. Peplowski[1].[1]Johns Hopkins University Applied Physics Laboratory, Laurel, MD 20723, USA.

Introduction: Distinctive low-reflectance material (LRM) was first observed on Mercury in Mariner 10 flyby images [1]. Visible to near-infrared reflectance spectra of LRM are flatter than the average reflectance spectrum of Mercury, which is strongly red sloped (increasing in reflectance with wavelength). From Mariner 10 and early MErcury, Surface, Space, ENvironment, GEochemistry, and Ranging (MESSENGER) flyby observations, it was suggested that a higher content of ilmenite, ulvöspinel, carbon, or iron metal could cause both the characteristic dark, flat spectrum of LRM and the globally low reflectance of Mercury [1,2]. Once MESSENGER entered orbit, low Fe and Ti abundances measured by the X-Ray and Gamma-Ray Spectrometers ruled out ilmenite and ulvöspinel as important surface constituents [3,4] and implied that LRM was darkened by a different phase, such as carbon or small amounts of micro- or nanophase iron or iron sulfide dispersed in a silicate matrix. Low-altitude thermal neutron measurements of three LRM-rich regions confirmed an enhancement of 1–3 wt% carbon over the global abundance, supporting the hypothesis that the darkening agent in LRM is carbon [5]. Here, using the final calibration of the Mercury Dual Imaging System (MDIS) 8-color global mosaic, we examine the distribution and spectral properties of LRM on a global scale, and extrapolate the results of Peplowski et al. [5] to place bounds on the carbon abundance of different LRM deposits across Mercury.

Distribution of Low Reflectance Material: LRM is distributed across Mercury, typically having been excavated from depth by craters and basins. In contrast to the brighter high reflectance plains (HRP) and smooth plains deposits, which exhibit morphological evidence of volcanism [e.g., 6-8], LRM is not associated with flow features or other evidence of a volcanic origin. Older LRM boundaries are generally diffuse, and grade into low-reflectance blue plains (LBP). Because of the common lack of sharp geologic boundaries, LRM has been defined primarily based on albedo and spectral shape, isolated through principal components (PC) analyses of MDIS color images [9]. LRM is the darkest material on Mercury, with an albedo of 4–5% at 560 nm (compared to a global 560-nm albedo of ~6%), and it exhibits a spectral slope that is substantially less red than the rest of Mercury. The low iron content of Mercury's surface results in a lack of the spectral absorption bands typically used to map mafic minerals on planets and asteroids. Thus, mathematical transformations such as PC analysis are required to map subtle spectral differences. For example, the second principal component (PC2), captures a combination of spectral slope and curvature, isolating LRM and hollows as one endmember, with red material and HRP as the other end member. LBP and intermediate plains (IP) are transitional from LRM to HRP [10]. In [5], concentrated LRM exposures were defined as regions with a photometrically corrected reflectance of <5% (at 560 nm wavelength) and a PC2 value of <0.023. This value corresponds with the lower ~25% of the range of PC2 values for the whole planet. The resulting LRM map, overlain on the global color mosaic, is shown in Fig. 1a. There are some regional concentrations where many moderate sized craters or several larger basins excavated LRM in close proximity to one another. LRM is most immediately recognizable visually when excavated by craters and deposited onto high-reflectance red plains (HRP, as in Caloris basin), due to the contrasting reflectance and spectral slopes of the different stratigraphic layers. However, it is also abundant throughout the oldest, rough terrains, where its boundaries are more difficult to delineate as they grade into LBP. In these older terrains LRM is still apparently associated with crater ejecta, but the high density of craters excavating LRM results in a patchy distribution of low-reflectance, low-PC2 material.

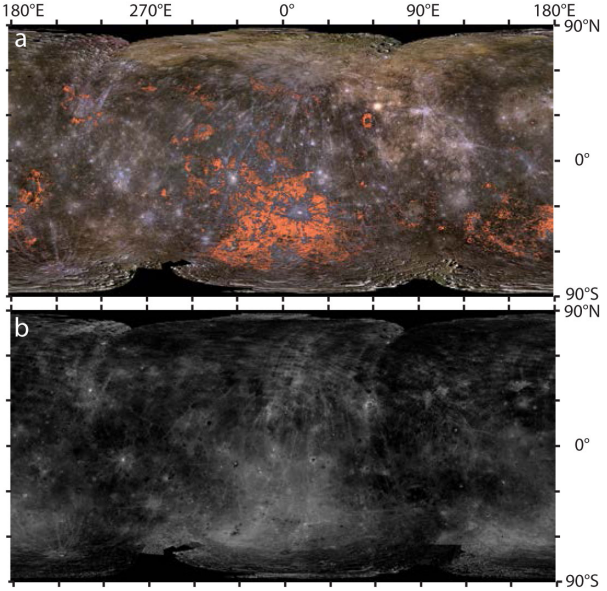

Fig. 1. (a) False color global map of Mercury with R=1000 nm, G=750 nm and B=430 nm. LRM shows up as dark bluish-black material, and grades into the slightly brighter LBP. The LRM map using albedo, PC2 and slope constraints as detailed in the text is overlain in orange. **(b)** ~600-nm broad band depth map.

Mapping LRM Directly: Because PC analyses are calculated using the spectral range over a given data set, a PC2 constraint cannot be directly translated to individ-

ual targeted color images, except in the rare case of images that contain the full range of Mercury's spectral diversity. The broad, shallow band near 600 nm that is observed in LRM (and often hollows material) can be isolated directly by dividing the planet as a whole by a reference spectrum and then calculating a band depth ratio. Murchie et al. [11] found that the most successful ratio for mapping the LRM was calculated by first dividing the full mosaic by a reference spectrum of the northern volcanic plains, and then calculating the ratio as:

$$\sim 600\ nm\ band\ depth = 1 - \left[\frac{(R560 + R630 + R750 + R830)/4}{(R900 + R480)/2}\right]$$

where R is photometrically corrected reflectance in each of the given filters. Although this ratio detected the broad, shallow curvature, calibration artifacts made it impossible to examine on a global scale. However, the newly calibrated 8-color mosaic [12] enables this feature to be directly mapped, and the map clearly highlights the same regions identified by the LRM map (Fig. 1b).

Extrapolating the Carbon content of LRM: In [5], 600-nm band depth ratio described above was found to correlate with abundance of carbon as measured during low-altitude neutron detector measurements. Although there were only three locations that could be measured, within uncertainty, there is a clear linear relationship between the average ~600 nm band depth for each LRM deposit (mapped using the PC constraints previously described) and the measured carbon content. Using the same methodology for calculating the band depths, and the same regions of interest used [5], we have recalculated the ~600 nm band depths for each of the regions using the new 8-color mosaic. Based on the derived band-depth to carbon relationship, we estimated carbon contents for other LRM deposits (Fig. 2). Our results suggest that some regions may contain as much as 5 wt% carbon above the global mean, a value consistent with the carbon content required to produce their low reflectances [11].

Carbon on Mercury: Two explanations for carbon on Mercury's surface had been proposed. The first suggests that carbon could be exogenic, delivered gradually by comets over Mercury's history [13]. The second is an endogenic origin, that any carbon that did not partition into the core of the planet would crystallize as graphite, and would have floated to the surface creating a primordial graphite flotation crust [14]. Across the surface of Mercury, LRM shows clear evidence of having been excavated from depth [9,11,15]. In cases where it is not clearly associated with specific craters, it occurs in patchy spots within broad regions of heavily cratered, ancient terrain where the ejecta from numerous small craters overlap [10,16]. This evidence, derived from global-scale mapping efforts, supports the hypothesis that this carbon is sourced from the remnants of a magma ocean flotation crust. However, the geophysical and geochemical implications of the carbon abundances measured from orbit and extrapolated to the planet as a whole are yet to be investigated. For example, if LRM is derived from a graphite flotation crust, what could be forming the hollows that are found in association with LRM? How thick and deep is the LRM layer, and if this were once a relatively pure graphite layer, how thick would it have been and how would it affect the thermal and chemical evolution of Mercury's magma ocean?

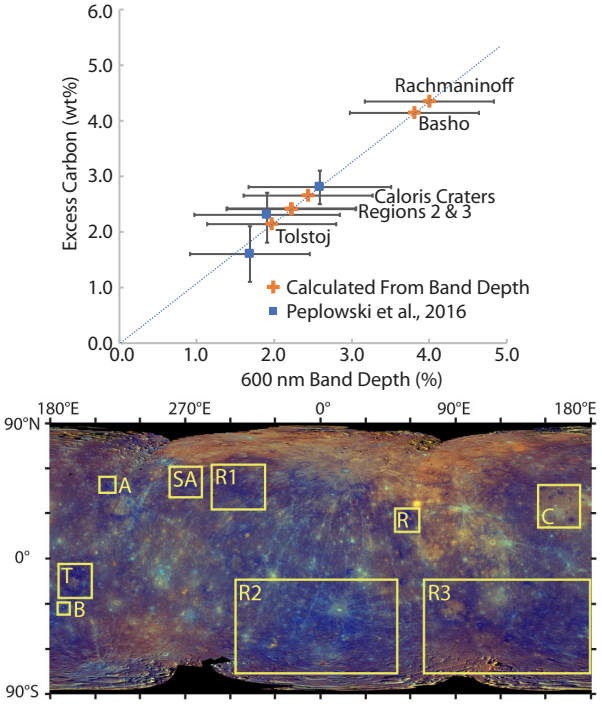

Fig. 2. (top) Extrapolated carbon content for different regions of the surface. Blue squares were measured directly in [5], orange plusses were calculated from the derived band depth relationship. **(bottom)** Enhanced color composite of Mercury with R=PC1, G=PC2, B=430/1000 nm slope. Locations of LRM-enriched craters measured in [5] A-Akutagawa, SA-Sholem-Aleichem, and R1-region LRM-A are shown, along with derived values for B-Basho, T-Tolstoj, R-Rachmaninoff and C-Craters within Caloris and two additional regional enhancements (R2, R3).

References: [1] Hapke, B. et al. (1975) *JGR* 80, 2431. [2] Robinson, M.S. et al. (2008) *Science* 321, 66. [3] Nittler, L.R. et al., (2011) *Science* 333, 1847. [4] Evans, R.G. et al. (2012) JGR 117, E00L07. [5] Peplowski, P.N. et al. (2016) *Nat. Geosci.* 9, 273-278. [6] Head, J.W. et al., (2011) *Science* 333, 1853–1856. [7] Whitten, J. L., et al. (2014) *Icarus* 241, 97-113. [8] Denevi, B.W. et al., (2013) *JGR Planets* 118, 891–907. [9] Klima, R.L., et al. (2016), *LPSC* 47, Abstract#1195. [10] Denevi, B. et al., (2016), *LPSC* 47, Abstract#1624. [11] Murchie, S.L. et al. (2015) *Icarus* 254, 287. [12] Denevi et al., (in press) DOI: 10.1007/s11214-017-0440-y. [13] Bruck Syal, M. et al. (2015), *Nat. Geosci.* 8, 352. [14] Vander Kaaden, K.E. and McCubbin, F.M. (2015) *JGR Planets* 120, 195. [15] Ernst, C.M. et al. (2015) *Icarus* 250, 413. [16] Leeburn et al. (2017), *LPSC* 48, Abstract#1964.

Acknowledgements: We are grateful to the NASA PMDAP program for supporting this work (#NNX14AM93G).